DIGITAL ACCESS TO SCHOLARSHIP AT HARVARD
DASH.HARVARD.EDU

HARVARD LIBRARY
Office for Scholarly Communication

X#Ray Reflectivity Studies of SiO\(_2\)/Si(001)

Citation
Rabedeau, T. A., I. M. Tidswell, Peter S. Pershan, J. Bevk, and B. S. Freer. 1991. X#ray reflectivity studies of SiO\(_2\)/Si(001). Applied Physics Letters 59(26): 3422-3424.

Published Version
doi:10.1063/1.105695

Permanent link
http://nrs.harvard.edu/urn-3:HUL.InstRepos:10357570

Terms of Use
This article was downloaded from Harvard University's DASH repository, and is made available under the terms and conditions applicable to Other Posted Material, as set forth at http://nrs.harvard.edu/urn-3:HUL.InstRepos:dash.current.terms-of-use#LAA

Share Your Story

The Harvard community has made this article openly available.
Please share how this access benefits you. Submit a story .

Accessibility

X-ray reflectivity studies of SiO_2/Si(001)

T. A. Rabedeau, I. M. Tidswell,[a] and P. S. Pershan
Department of Physics and Division of Applied Science, Harvard University, Cambridge, Massachusetts 02138

J. Bevk and B. S. Freer
AT&T Bell Laboratories, Murray Hill, New Jersey 07974

(Received 22 July 1991; accepted for publication 26 September 1991)

X-ray reflectivity has been utilized in a study of the SiO_2/Si interfacial structure for dry oxides grown at room temperature on highly ordered Si(001) surfaces. Scattering near (± 110) demonstrates the Si lattice termination of the wafers studied is characterized by a highly ordered array of terraces separated by monoatomic steps. Specular reflectivity data indicate the "native" dry oxide thickness is approximately 5 Å with a 1-Å vacuum interface width. Residual laminar order in the oxide electron density along the oxide/Si interfacial normal decays exponentially from the oxide/Si interface with a ~2.7-Å decay length.

Widespread interest in the structure of the SiO_2/Si(001) interface stems both from the crucial role this interface plays in electronic device performance and from the fundamental importance of understanding the chemistry and physics of semiconductor oxidation. Despite extensive and sustained experimental effort, characterization of the SiO_2/Si interfacial structure remains incomplete. It is well established that oxides grown on Si(001) are structurally amorphous, stoichiometric SiO_2 to within ~7 Å of the SiO_2/Si interface; however, definitive characterization of the structural evolution from Si crystalline order to amorphous SiO_2 is lacking. Recently, grazing incidence x-ray scattering,[1-4] reflection-high-energy-electron diffraction (RHEED)[5] and high-resolution transmission electron microscopy[5-7] have been utilized to study the SiO_2/Si(001) interfacial structure. Each of these studies has focused primarily on order in the plane of the interface and the decay of this in-plane order away from the interface. The existence of the truncated Si lattice, however, can induce laminar order in the oxide along the interfacial normal even in the absence of in-plane order. Since the extent and perfection of in-plane order at the interface are disputed, it is essential to establish the decay of oxide order along the interfacial normal independent of the degree of in-plane order. X-ray specular reflectivity probes the interfacial normal order of the $G_{xy} = (00)$ Fourier component of the electron density (x,y in the plane of the interface); hence, it provides the requisite sensitivity to interfacial normal order even in the presence of in-plane disorder.

In this Letter we present results of an x-ray reflectivity study of interfacial order in dry oxides grown at room temperature on well oriented, molecular-beam epitaxy (MBE) prepared Si(001) surfaces. Characterization of the Si lattice termination as a highly ordered array of terraces separated by monoatomic steps with the mean terrace size determined by the wafer miscut is obtained by analyzing x-ray scattering near (± 110).[8] X-ray specular reflectivity is utilized to establish the oxide thickness, vacuum interface width, and decay of oxide order along the SiO_2/Si interfacial normal.

The wafers employed in this study were aligned to within 0.05° of the [001] crystallographic axis. Following evaporative removal of a protective Shiraki oxide, residual disorder in the Si lattice termination was healed through a combination of Si MBE deposition and thermal annealing. Oxides were formed in the vacuum chamber by exposing room-temperature wafers to dry oxygen at 1-atm pressure for 12 h (wafer 1) or similar dry oxidation for two weeks (wafer 2). X-ray scattering measurements were conducted at the National Synchrotron Light Source (NSLS) on beam lines X20A and X22B in a vertical scattering geometry using doubly focused radiation of 1.54–1.57-Å wavelength. To prevent uncontrolled wet oxidation, the wafers were maintained continuously in a dynamic vacuum (2×10^{-9} Torr) throughout transport and during the x-ray measurements.

The x-ray scattering observed in transverse scans at (± 110) for wafer 1 is presented in Fig. 1. Scattering at (± 110) is forbidden for an infinite Si crystal; however, truncation of the Si lattice results in diffuse rods of scattering extending in reciprocal space along the interfacial normal away from the bulk diffraction peaks.[9,10] Since the crystal is slightly miscut from the [001] crystallographic axis, rods emanating from the ($\pm 1\ 1\ \pm 1$) Bragg peaks do not coincide at (± 110), resulting in the two principal maximum observed in each of the transverse scans of Fig. 1. The secondary maxima apparent in Fig. 1 are an indication that the lattice termination is characterized by an ordered terrace structure[11] which is the microscopic manifestation of the crystallographic miscut.

Electron scattering from stepped surfaces has been discussed by several authors.[11-13] The formalism developed for electron scattering is applicable to the x-ray scattering case provided the scattering factor for the truncated column of scatterers is explicitly included.[14] Since [001] is a fourfold screw axis for Si there are two types of lattice terminations (denoted A and B) which are related by a 90° rotation about the [001] axis. At (110) the scattering factor for a column of scatterers with a B termination vanishes while that of the A termination is nonvanishing.[15] At (-110) the situation is reversed. Using the formalism of Pukite *et al.*,[11] the scattering cross section for a terraced structure with monoatomic steps[16] can be written

[a]Present address: Lawrence Berkeley Laboratory, Berkeley, CA 94720.

 0003-6951/91/513422-03$02.00 © 1991 American Institute of Physics

Downloaded 12 Oct 2010 to 128.103.149.52. Redistribution subject to AIP license or copyright; see http://apl.aip.org/about/rights_and_permissions

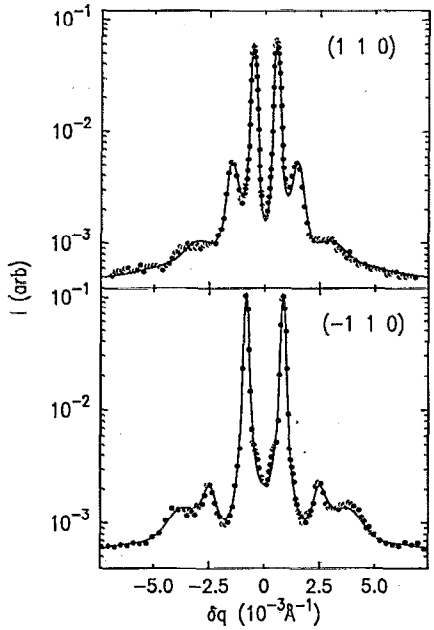

FIG. 1. Scattering at (± 110) for wafer 1 (●). The different peak separations at (110) relative to those at (-110) result from spectrometer resolution and scan trajectory effects. The lines represent the results of the fit to the terrace ordering model.

$$\frac{d\sigma}{d\Omega}(110) \sim \frac{|F_A|^2}{\delta q_n^2 l_A} \mathrm{Re}\left[\frac{(1-P_A)(1+P_B S_\pm^2)}{(1+P_A P_B S_\pm^2)}\right], \qquad (1)$$

where this form is derived by approximating the actual terrace structure as a series of terraces with straight edges and the size of any individual terrace is assumed statistically independent of the size of all other terraces.[11] F_A is the scattering factor for a column of scatterers ending in an A-type termination, δq_n is the in-plane momentum transfer along $\hat{n}$ measured relative to (110) [i.e.,$\delta q_n = (\mathbf{q} - \mathbf{G}_{110})\cdot\hat{n}$] where $\hat{n}$ is the in-plane unit vector normal to the terrace edges, l_A is the average type A terrace size, P_A and P_B are the Fourier transforms with respect to δq_n of the A and B terrace size distributions, $S_\pm = S_+ - S_-$, and $S_+ (S_-)$ is the probability of a step up (down). At (-110) the scattering cross section is identical to Eq. (1) with A and B interchanged and $\delta q_n = (\mathbf{q} - \mathbf{G}_{-110})\cdot\hat{n}$.

The solid lines shown in Fig. 1 depict the results of a simultaneous fit to both transverse scans to the form of Eq. (1) after convolution with the spectrometer resolution function and using Gaussians to represent the terrace size distributions (i.e., $P_A = e^{i\delta q_n l_A} e^{-\delta q_n^2 \sigma_A^2/2}$). The Gaussian terrace size distribution parameters determined from the fit are $l_A = 1480 \pm 30$ Å, $l_B = 1760 \pm 35$ Å, $\sigma_A = 300 \pm 30$ Å, $\sigma_B = 470 \pm 50$ Å, and $S_+ = 0.994 \pm 0.006$. The projection of the miscut into the [100]×[010] crystallographic plane (i.e., $\hat{n}$) is $1.6 \pm 1.0°$ towards [100] from [010]. Comparable quality fits were obtained using exponential terrace distributions with similar values for l_A, l_B and the miscut projection and $\sigma_A = 240 \pm 25$ Å, $\sigma_B = 370 \pm 40$ Å, and $S_+ = 1.00 + 0.0/ - 0.006$. Regardless which functional form is utilized to represent the terrace size distribution, it is apparent the Si lattice termination is accurately described as an ordered array of large terraces separated by monoatomic steps with the average terrace size determined by the wafer miscut. We believe the perfection of the order in this terrace structure reflects the MBE preparation of the Si surface prior to oxidation rather than an intrinsic property of SiO_2/Si interfaces.

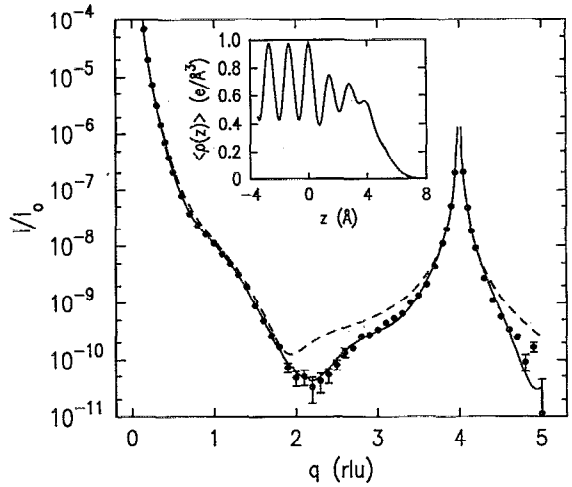

FIG. 2. Absolute scattering intensity along the specular rod (●) for wafer 1. The solid (broken) line represents the results of the fit to the model with (without) a laminar oxide component. The inset depicts the average electron density along the crystal normal as determined from the fit represented by the solid line. The Si lattice extends for $z \leq 0.0$.

X-ray specular reflectivity data collected from wafer 1 are depicted in Fig. 2. The absolute reflectivity approaches 1.0 at small momentum transfer (not shown) as expected for a semi-infinite medium. The reflectivity data were collected with the wafer [100] axis in the scattering plane such that the staircase of terraces resulting from the miscut ascends in the direction perpendicular to the scattering plane. Since the spectrometer resolution is very coarse in this direction (100 Å typical coherence length) the observed specular scattering does not result from the coherent interference of scattered fields from adjacent terraces. Thus any interfacial normal order invoked to explain the specular reflectivity data represents the average order along the interfacial normal of any one average terrace and *not* an effect associated with the steps in the lattice termination level.

The specular reflectivity data were fit by comparing the measured scattering with that calculated for a model system. The model system consists of an abruptly truncated Si lattice with the oxide electron density represented by two components: ordered along the interfacial normal (i.e., laminar order) and amorphous. The laminar component decays exponentially away from the SiO_2/Si interface. This component is embedded in a smoothly varying amorphous component such that the average total electron density in any oxide layer is constant until the oxide terminates at the vacuum interface. In the Born approximation the reflectivity is given by the expression[17]

Downloaded 12 Oct 2010 to 128.103.149.52. Redistribution subject to AIP license or copyright; see http://apl.aip.org/about/rights_and_permissions

TABLE I. Parameters from the best fits to the specular reflectivity data of wafers 1 and 2. ρ_0 is scaled by the electron density of crystalline Si, d_{oxide} is the oxide thickness, and σ_{vacuum} is the oxide/vacuum interface width. The χ^2's were determined using counting statistics to represent the reflectivity data uncertainty.

Parameter	Wafer 1	Wafer 2
ρ_0/ρ_{Si}	0.86	0.89
d_{oxide}	4.93 Å	4.57 Å
σ_{vacuum}	0.95 Å	1.08 Å
D	2.85 Å	2.46 Å
d_1	1.37 Å	1.35 Å
d_2	1.36 Å	1.31 Å
d_3	1.16 Å	1.19 Å
χ^2	5.0	3.2

$$\frac{I(q)}{I_0}=\frac{16\pi^2 r_e^2 P(q)}{a^4 q^2}\left|\frac{2f_{\text{Si}}e^{-q^2\langle u^2\rangle/2}}{1-e^{-iqa/4}}+\sum_{n=1}^{\infty} bf_{\text{Si}} \times e^{-q^2\langle u_n^2\rangle/2}e^{(iq-1/D)\Sigma_{j=1}^{n}d_j}+a^2\int \rho_a(z)e^{iqz}\,dz\right|^2 \quad (2)$$

where I_0 denotes the incident flux, r_e is the Thompson radius, $P(q)$ represents a polarization correction, a is the Si lattice constant (5.431 Å), q is the momentum transfer along the surface normal, f_{Si} is the Si atomic form factor, and $e^{-q^2\langle u^2\rangle/2}$ is the crystalline Si Debye-Waller factor. The term proportional to $1/(1-e^{-iqa/4})$ results from the truncated Si lattice. The sum over n represents the scattering from the exponentially decaying ordered oxide with characteristic decay length D. The scaled Si atomic form factor bf_{Si} represents the effective atomic form factor of the ordered oxide and the Debye-Waller term $e^{-q^2\langle u_n^2\rangle/2}$ approximates the effect of static disorder on the reflectivity. The final term denotes the scattering from the amorphous component of the oxide where the amorphous electron density $\rho_a(z)$ has the following properties. The interface between the amorphous oxide and vacuum is described by an error function profile. Away from the vacuum interface, the *total* average electron density in any oxide layer n is constant (ρ_0) with the average *amorphous* electron density in the layer given by $\rho_0-[bf_{\text{Si}}(q=0)e^{-(\Sigma_{j=1}^{n}d_j)/D}]/d_n a^2$. Within a given layer $\rho_a(z)$ varies linearly (subject to the constraint on the layer average amorphous density) such that $\rho_a(z)$ is continuous.

The results of the best fit to the reflectivity data of wafer 1 are depicted as the solid line in Fig. 2. The parameters determined from this fit and a fit to the specular reflectivity data of a second wafer dry oxidized for two weeks are listed in Table I. The number of ordered oxide layers was restricted to three owing to the thinness of the oxide; however, inclusion of a fourth layer does not substantially alter the results. The Debye–Waller factor $\langle u_n^2\rangle^{1/2}$ was fixed at 0.2 Å and the scale factor b was fixed at 2 which is roughly the expected value for a perfectly ordered oxide. The uncertainties in the tabulated fitting parameters are typically less than the intersample variation. These fits indicate the thickness of native dry oxides is substantially less than the ~15-Å thickness of typical native oxides formed by air oxidation. The residual laminar order in the oxide decays with a ~2.7-Å characteristic decay length. The necessity of including residual laminar order in the oxide is illustrated in Fig. 2 where the broken line depicts the results of the best fit to a model consisting of an abruptly terminated Si lattice with only an amorphous oxide overlayer ($\chi^2=97$). While these data do not address the characteristic length for stoichiometric evolution, the clear evidence for a nonzero decay length for laminar order in the oxide indicates the crystalline Si to amorphous SiO_2 transition is not abrupt. Given the sensitivity of electron mobilities to the SiO_2/Si interface width, this diffuse character of the interface should be considered in calculations of the electronic properties of the interface.

To recapitulate, the SiO_2/Si interfacial structure for dry oxides grown on highly ordered Si(001) surfaces has been investigated by x-ray reflectivity. Scattering at ($\pm$110) indicates the Si lattice termination is characterized by an ordered terrace array with monoatomic steps at the terrace edges. Analysis of specular reflectivity data shows the native dry oxide is ~5-Å thick with 1-Å vacuum interface width. Residual laminar order along the oxide/Si interface normal decays exponentially into the oxide from the oxide/Si interface with a ~2.7-Å decay length.

The authors acknowledge discussions with P. H. Fuoss and G. Renaud. This work was supported by DOD JSEP Grant No. N00014-89-J-1023. NSLS is supported by DOE Contract No. DE-AC02-76CH00016.

[1] P. H. Fuoss, L. J. Norton, S. Brennan, and A. Fischer-Colbrie, Phys. Rev. Lett. **60**, 600 (1988).
[2] G. Renaud, P. H. Fuoss, A. Ourmazd, J. Bevk, B. S. Freer, and P. O. Hahn, Appl. Phys. Lett. **58**, 1044 (1991).
[3] T. A. Rabedeau, I. M. Tidswell, P. S. Pershan, J. Bevk, and B. S. Freer, Appl. Phys. Lett. **59**, 706 (1991).
[4] I. Hirosawa, K. Akimoto, T. Tatsumi, J. Mizuki, and J. Matsui, J. Cryst. Growth **103**, 150 (1990).
[5] F. Rochet, M. Froment, C. D'Anterroches, H. Roulet, and G. Dufour, Philos. Mag. B **59**, 339 (1989).
[6] A. Ourmazd, D. W. Taylor, J. A. Rentschler, and J. Bevk, Phys. Rev. Lett. **59**, 213 (1987).
[7] J. M. Gibson and M. Y. Lanzerotti, Nature **340**, 128 (1989).
[8] Momentum transfers are reported in bulk Si reciprocal lattice units (1 rlu = 1.157 $Å^{-1}$) unless noted.
[9] I. K. Robinson, Phys. Rev. B **33**, 3830 (1986).
[10] S. R. Andrews and R. A. Crowley, J. Phys.C **18**, 6427 (1985).
[11] P. R. Pukite, C. S. Lent, and P. I. Cohen, Surf. Sci. **161**, 39 (1985).
[12] M. Henzler, Surf. Sci. **73**, 240 (1978).
[13] J. M. Pimbley and T.-M. Lu, Surf. Sci. **159**, 169 (1985).
[14] E. Vlieg, J. F. van der Veen, S. J. Gurman, C. Norris, and J. E. MacDonald, Surf. Sci. **210**, 301 (1989).
[15] X-ray grazing incidence diffraction data from wafer 1 indicate the presence of weak 2×1 order at the SiO_2/Si interface. Measurements of the absolute scattering cross section of the 2×1 order demonstrate the interfacial coverage is only ~10% and the structure is rather disordered. (See Ref. 3 for details). Consequently, the contribution of this structure to the total scattering factor at ($\pm$110) is small and, for simplicity, we disregard it.
[16] Biatomic steps were not included since *room-temperature* oxidized Si(001) wafers miscut 0.05° towards [010] do not exhibit biatomic steps. G. Renaud and P. Fuoss (private communication). See also O. L. Alerhand, A. N. Berker, J. D. Joannopoulos, D. Vanderbilt, R. J. Hamers, and J. E. Demuth, Phys. Rev. Lett. **64**, 2406 (1990); T. W. Poon, S. Yip, P. S. Ho, and F. F. Abraham, *ibid.* **65**, 2161 (1990).
[17] D. Gibbs, B. M. Ocko, D. M. Zehner, and S. G. J. Mochrie, Phys. Rev. B **38**, 7303 (1988).

Downloaded 12 Oct 2010 to 128.103.149.52. Redistribution subject to AIP license or copyright; see http://apl.aip.org/about/rights_and_permissions